Sergei Rudenko, Karl-Hans Neumayer, Denise Dettmering, Saskia Esselborn, Tilo Schöne, and Jean-Claude Raimondo: **Improvements in Precise Orbits of Altimetry Satellites and Their Impact on Mean Sea Level Monitoring,** *IEEE Transactions on Geoscience and Remote Sensing*, Volume 55, Issue 6, pp. 3382 - 3395, June 2017.

DOI: https://doi.org/10.1109/TGRS.2017.2670061

Improvements in precise orbits of altimetry satellites and their impact on mean sea level monitoring

Sergei Rudenko, Karl-Hans Neumayer, Denise Dettmering, Saskia Esselborn, Tilo Schöne, and Jean-Claude Raimondo

***Abstract*—New, precise, consistent orbits (VER11) of altimetry satellites ERS-1, ERS-2, TOPEX/Poseidon, Envisat, Jason-1 and Jason-2 have been recently derived at GFZ German Research Centre for Geosciences in the extended ITRF2008 terrestrial reference frame using improved models and covering the time span 1991–2015. These orbits show improved quality, as compared to GFZ previous (VER6) orbits derived in 2013. Improved macromodels reduce root mean square (RMS) fits of satellite laser ranging (SLR) observations by 2.6, 6.9 and 7.0% for TOPEX/Poseidon, Jason-1 and Jason-2, respectively. Applying Vienna Mapping Functions 1 instead of Hopfield model for tropospheric correction of Doppler Orbitography and Radiopositioning Integrated by Satellite (DORIS) observations reduces RMS fits of SLR observations by 2.0-2.4% and those of DORIS observations by 2.6% for Envisat and Jason satellites. Using satellite true attitude instead of models improves Jason-1 SLR RMS fits by 41% from July 2012 until July 2013. The VER11 orbits indicate the mean values of the SLR RMS fits between 1.2 and 2.1 cm for the different missions. The internal orbit consistency in the radial direction is between 0.5 and 1.9 cm. The global mean sea level trend for the period 1993 to 2014 from TOPEX, Jason-1 and Jason-2 is increased by 0.2 mm/year to 3.0 mm/year from the GFZ VER6 to VER11 orbits. Regionally, the decadal trends from GFZ VER11 and external orbits vary in the order of 1 mm/year.**

***Index Terms*—altimetry analysis; altimetry satellite; DORIS; low earth orbit satellites; orbit determination; orbital calculations; satellite attitude; satellite laser ranging (SLR); sea level**

I. Introduction

PRECISE orbits of altimetry satellites are a basis for all kinds of altimetry-based oceanographic applications, such as investigations of global and regional mean sea level changes, climate change, generation of mean sea surface height models, ocean tide modelling and other applications. They are extremely important for long-term investigations, since they realize the reference for the altimetry measurements. Precise orbits of some of these satellites are required to generate accurate baselines for Interferometric Synthetic Aperture Radar (InSAR) data processing to generate maps of surface deformation or digital elevation. Satellite orbits are applied also for the validation of various background models and processing algorithms used for orbit determination.

Orbits of various altimetry satellites have been computed by different groups. Thus, precise orbits of the European Remote Sensing Satellites ERS-1 and ERS-2 were derived by [32] in the ITRF2005 [2] terrestrial reference frame using the models based mainly on the International Earth Rotation and Reference Systems Service (IERS) Conventions 2003 [27]. The orbits show 2–3 cm accuracy in the radial direction. Precise orbits of TOPEX/Poseidon and Jason-1 were computed by [4] in the ITRF2005 reference frame using satellite laser ranging (SLR) and DORIS (Doppler Orbitography and Radiopositioning Integrated by Satellite) observations, the GGM02C gravity field model [37] and other models based mainly on the IERS Conventions 2003. A radial accuracy of these orbits is 1.5 to 2.0 cm. This resulted in the creation of a new version of the geophysical data records (GDR) standards, namely, GDR-C standards [10] based on the IERS Conventions 2003, ITRF2005 terrestrial reference frame, EIGEN-GL04S [23] geopotential model, and other models.

The difference of the next (GDR-D) version [28] of the GDR standards with respect to (w.r.t.) GDR-C ones consists in applying extended ITRF2008 terrestrial reference frame that makes use of SLRF2008 [29], DPOD2008 [39] and IGS08 [31]. ITRF2008 [3] contains additionally 57 SLR and 15 DORIS stations and is derived using three more years (2006-2009) of DORIS data and 13 more years (1983-1993 and 2006-2009) of SLR data, as compared to ITRF2005. This allows to determine station positions and velocities and, as a result, satellite orbits more precisely. The other main differences of the GDR-D standards w.r.t. GDR-C ones consist of using the EIGEN-GRGS_RL02bis_MEAN-FIELD Earth's gravity field model, Biancale and Bode [5] model for atmospheric tides, Earth orientation data consistent with the IERS Conventions 2010 [19] and ITRF2008, pole tide [19], and the empirical Global Pressure and Temperature (GPT) model [7] and Global Mapping Function (GMF) [6] for DORIS troposphere correction. The GFZ version 6 (VER6) orbits of ERS-1, ERS-2, Envisat and TOPEX/Poseidon [33] were derived in 2013 applying the models that are consistent with the GDR-D

Manuscript received September 12, 2016; revised December 7, 2016. This research was partly supported by the European Space Agency (ESA) within the Climate Change Initiative Sea Level (SLCCI) Phase II project and by German Research Foundation (DFG) within the projects "Consistent dynamic satellite reference frames and terrestrial geodetic datum parameters", "Interactions of low-orbiting satellites with the surrounding ionosphere and thermosphere (INSIGHT)" and "Coastal and regional sea level change and subsidence - the hazardous potential in Indonesia and South East Asia (CoRSEA)". *(Corresponding author: Sergei Rudenko.)*

S. Rudenko was with Helmholtz Centre Potsdam – GFZ German Research Centre for Geosciences, 14473 Potsdam, Germany, now at Deutsches Geodätisches Forschungsinstitut der Technischen Universität München (DGFI-TUM), 80333 Munich, Germany (e-mail: sergei.rudenko@tum.de).

K.-H. Neumayer, S. Esselborn and T. Schöne are with Helmholtz Centre Potsdam – GFZ German Research Centre for Geosciences, 14473 Potsdam, Germany (e-mail: neumayer@gfz-potsdam.de, Saskia.Esselborn@gfz-potsdam.de, tschoene@gfz-potsdam.de).

D. Dettmering is with Deutsches Geodätisches Forschungsinstitut der Technischen Universität München (DGFI-TUM), 80333 Munich, Germany (e-mail: denise.dettmering@tum.de).

J.-C. Raimondo is with SpaceTech GmbH, 88090 Immenstaad, Germany (e-mail: raimondo@gfz-potsdam.de).

orbit standards, except the DORIS troposphere correction, for which the Hopfield [18] model was used. Since orbit errors remain to be one of the major error sources for global and regional sea level products [1], further improvement of the orbit quality for altimetry satellites remains a very important task.

In this paper, we discuss further improvements in precise orbit determination of altimetry satellites (Section II), as compared to the GFZ VER6 orbits. In particular, we investigate the impact of using satellite true attitude provided by quaternions derived from star tracker observations for Jason-1 and Jason-2 instead of models on satellite orbits (Section II-A), show the influence of the improvements in TOPEX/Poseidon, Jason-1 and Jason-2 satellite macromodels on the orbit quality (Section II-B), and the impact of tropospheric correction models for DORIS observations, in particular, the impact of applying the Vienna Mapping Functions 1 (VMF1) instead of the Hopfield model (Section II-C). Some other updates in altimetry satellite orbit modelling are discussed in Section II.

We present GFZ version 11 (VER11) orbits of six altimetry satellites (ERS-1, ERS-2, TOPEX/Poseidon, Envisat, Jason-1 and Jason-2) derived recently by applying improved models consistent with the GDR-E standards [28] in the extended ITRF2008 reference frame. The orbits have been derived using 'Earth Parameter and Orbit System – Orbit Computation' (EPOS-OC) software [41] developed at GFZ.

The rest of the paper is organized as follows. The updates and improvements in precise orbit determination are discussed in Section II. The main results on the GFZ VER11 orbits derived using the improved models as compared to the GFZ VER6 orbits are provided in Section III-A. The results of the quality assessment of the GFZ VER11 orbits employing single-satellite altimetry crossover analysis (Section III-B) and multi-mission crossover analysis (Section III-C) are also presented. The orbit quality assessment based on sea level anomalies is given in Section III-D. Effects of the orbit choice on global and regional sea level trends are discussed in Section IV. Finally, conclusions are drawn (Section V).

II. Updates and improvements in precise orbit determination

The background models for orbit determination and processing algorithms used to derive the GFZ VER11 orbits are based on those applied for the VER6 orbits [33]. The orbit of ERS-1 is derived using SLR data and single-satellite altimetry crossover data (SXO) data computed applying GFZ's Altimeter Database and Processing System (ADS, [36]), whereas precise range and range-rate (PRARE) data are employed additionally for ERS-2. The orbits of TOPEX/Poseidon, Envisat and two Jason satellites are derived using SLR and DORIS data. SLR and DORIS data are used from the International Laser Ranging Service (ILRS, [30]) and the International DORIS Service (IDS, [38]), respectively. Orbits of ERS-1, ERS-2 and Envisat are derived at 7-day orbital arcs, whereas orbits of TOPEX/Poseidon, Jason-1 and Jason-2 are computed at 12-day orbital arcs allowing two-day arc overlaps for each satellite, except the cases when orbit manoeuvres took place. All orbital arcs are manoeuvre-free. The RMS fits of observations given in this paper are computed for the observations used in orbit determination with the satellite elevation angle more than 10°.

We make use of the extended ITRF2008 terrestrial reference frame realization. Polar motion and UT1 are applied according to the IERS EOP 08 C04 (IAU2000A) series[1]. The precession and nutation model, solid Earth and pole tides are modelled according to the IERS Conventions 2010 [19]. Atmospheric tides are computed according to [5]. The third body gravitational perturbations are computed for the Sun, the Moon and eight major planets using DE-421 planetary ephemerides [17].

Additionally, some models and input data have been updated and improved (Table I). Thus, based on the results obtained by [34] we use reprocessed release 05 (RL05) of the AOD1B product. This allows us to improve orbit quality, as described by [34]. Additionally, we increase the truncation level of the AOD1B expansion from 50 to 100. The maximum differences of Envisat positions adjusted at 7-day orbital arcs using SLR and DORIS observations are less than 1, 4 and 3.5 mm in the radial, cross-track and along-track directions, respectively, when applying the truncation degree 50 and 100 of the AOD1B RL05 product.

Using EIGEN-6S4 time variable Earth's gravity field model [16] has minor impact on the satellite orbits of question, as compared to EIGEN-6S2 [33]. Thus, in case of ERS-1 orbit at the time interval from 1 August 1991 until 5 July 1996, it reduces the mean values of SLR and SXO RMS fits, cross- and along-track arc overlaps by 0.3, 0.1, 2.0, and 0.3%, respectively, and increases the mean value of radial overlaps by 0.1%. At the same time, the mean values of SLR RMS fits slightly (by 0.2–0.3%) increase for five other satellites.

Applying the EOT11a global empirical ocean tide model EOT11a [35] instead of the EOT10a model [26] for orbit determination of the altimetry satellites studied by us has also minor impact on the residuals. Thus, the mean values of SLR RMS fits decrease by 0.14% for Envisat and by 0.04% for Jason-1, but increase by 0.04% for ERS-1 and 0.19% for ERS-2 over the whole duration of each mission and do not change notably for TOPEX/Poseidon.

Tidal geocenter variations are modelled by ocean tide and atmospheric pressure loading. No explicit model for non-tidal geocenter motion is used. Possible mismodelling is absorbed by estimated parameters, such es range and time biases and troposphere refraction coefficients. The GFZ atmospheric loading corrections for station coordinates are computed using in-house program allowing the computation of the site displacements due to atmospheric loading based on the [13] theory using the Love numbers from Gegout (1997, private communication). The 6-hour reanalysis (ERA-Interim) surface pressure data from the European Center for Medium-Range Weather Forecasts (ECMWF) are developed in spherical harmonics and convoluted with associated Legendre functions to yield the site displacements.

We have improved parametrization at some orbital arcs having observation gaps trying to reduce outliers in the ob-

[1] https://www.iers.org/IERS/EN/DataProducts/EarthOrientationData/eop.html

TABLE I
THE MAIN DIFFERENCES IN THE MODELS USED TO DERIVE THE GFZ VER11 ORBITS, AS COMPARED TO THOSE APPLIED FOR THE GFZ VER6 ORBITS. THE WORD 'YES' INDICATES THAT THE MODEL WAS USED FOR THE SPECIFIC SATELLITE (ERS-1, ERS-2, ENVISAT, TOPEX, JASON-1 AND JASON-2).

The differences / Satellites	ERS-1	ERS-2	Envisat	TOPEX	Jason-1	Jason-2
Replacement of AOD1B RL04 by AOD1B RL05 reprocessed	Yes	Yes	Yes	Yes	Yes	Yes
AOD1B truncation level of the spherical harmonic coefficients: 100 instead of 50	Yes	Yes	Yes	Yes	Yes	Yes
Improvement of parametrization at some orbital arcs	Yes	Yes	Yes	Yes	Yes	Yes
Use of the VMF1 instead of the Hopfield model for DORIS tropospheric correction			Yes	Yes	Yes	Yes
EIGEN-6S4 geopotential model (instead of EIGEN-6S2 model)	Yes	Yes	Yes	Yes	Yes	Yes
Use additionally DORIS data at some time spans (Envisat, April-June 2002)			Yes			
Correction of DORIS data for South Atlantic Anomaly (2002–2013)					Yes	
Ocean tide model: EOT11a (instead of EOT10a)	Yes	Yes	Yes	Yes	Yes	Yes
An updated station file (more SLR and DORIS stations)	Yes	Yes	Yes	Yes	Yes	Yes
Atmospheric loading based on ECMWF ERA-Interim data (instead of operational data)	Yes	Yes	Yes	Yes	Yes	Yes
An updated file for ocean loading for station coordinates	Yes	Yes	Yes	Yes	Yes	Yes
EOP 08 C04 Earth Orientation Parameters (as of 4 May 2015)	Yes	Yes	Yes	Yes	Yes	Yes
An improved satellite macromodel				Yes	Yes	Yes
Estimation of the global scaling factor of the solar radiation pressure model					Yes	Yes
Using true (observed) satellite attitude instead of an attitude model					Yes	Yes

servation residuals and RMS of crossover differences. This was done by increasing or decreasing by the coefficient 2 the time step of the atmospheric drag coefficients and empirical cross-track and along-track accelerations estimated once per revolution by the least square adjustment. The list of the estimated parameters at each orbital arc is given in Table II.

We use, additionally to SLR data, DORIS data for Envisat also in April – June 2002. Therefore, Envisat GFZ VER11 orbit is derived using both SLR and DORIS data during the whole mission from 12 April 2002 until 8 April 2012. This makes the Envisat orbit consistent and improves Envisat VER11 orbit quality for April – June 2002, as compared to the VER6 orbit resulting in the reduction of the RMS of the crossover differences by about 1 mm (1.7%) for this period.

The ocean loading corrections for station coordinates are computed applying in-house program using the convolution of Green functions with gridded amplitudes and phases of tidal constituents for a given site location based on the FES2004 [24] ocean tide model.

The oscillators of four DORIS satellites (Jason-1, Jason-2, Jason-3 and SPOT-5) are affected by the South Atlantic Anomaly (SAA) caused by the Earth's inner Van Allen radiation belt. DORIS data corrected for the SAA using the [22] model are employed for Jason-1 for the whole duration (2002–2013) of the mission. The SAA effect on Jason-2 is about 90% smaller than on Jason-1 [40], is mainly on the positions, when estimated, of the SAA-affected stations rather than on the orbit, and therefore is not modelled by us. No Global Positioning System (GPS) satellites are known to be affected by the SAA, since they do not enter this radiation belt.

Additionally, a station file as well as a file for ocean loading for station coordinates has been updated for the period from April 2012 until April 2015. This allows using more SLR and DORIS stations.

A. Impact of true attitude modelling for Jason-1 and Jason-2 on satellite orbits

We first give a brief description how the attitude modelling for Jason-1 and Jason-2 has been done up to now inside the EPOS-OC processing package. We then explain how the incorporation of real-world star-tracker camera data has been achieved. It is shown further below that the orbit quality of both Jason-1 and Jason-2 benefits from this change in the processing strategy. In the case of Jason-1 the improvement is considerable.

By default, the satellites Jason-1, Jason-2 and TOPEX are handled inside the EPOS-OC more or less in the same manner.

Let ξ, $\dot{\xi}$ be the three-dimensional vectors that give the position and velocity of the satellite in the Conventional Inertial System (CIS). Let η_{CIS} and η_{SAT} be the three-dimensional coordinate vectors of one and the same point in the CIS frame and the satellite body system (SAT), respectively. It is then true that

$$\eta_{CIS} = \left(\begin{array}{ccc} \mathsf{T}, & \text{-}\mathsf{N}, & \text{-}\mathsf{R} \end{array} \right) R_3(-\Psi)\ \eta_{SAT} \tag{1}$$

where the three-dimensional column vectors R, T, N, indicating *radial*, *tangent* and *normal*, are defined according to

$$\mathsf{R} = \frac{\xi}{\|\xi\|_2}, \quad \mathsf{N} = \frac{\xi \times \dot{\xi}}{\left\|\xi \times \dot{\xi}\right\|_2}, \quad \mathsf{T} = \mathsf{N} \times \mathsf{R}. \tag{2}$$

and where $R_3(t)$ is the orthogonal matrix of a rotation around the z-axis, defined in the usual manner

$$R_3(t) = \begin{pmatrix} \cos(t) & \sin(t) & 0 \\ -\sin(t) & \cos(t) & 0 \\ 0 & 0 & 1 \end{pmatrix} \tag{3}$$

The yaw angle Ψ depends on the orientation of the Sun w.r.t. the orbit plane. Together with an appropriate rotation of the solar panel w.r.t. the satellite body it ensures that the solar cells are always oriented towards the Sun in an optimal manner. The explicit form of Ψ is somewhat involved. It will not be derived here as a formula, the interested reader is referred to [11, Fig. 3, p. 14]. Instead, the following informal description shall suffice.

Yaw steering mode can be explained in the following way. Imagine that the satellite had a steering pilot, looking in flight direction, his spine is aligned with the height direction. In this nominal orientation, the satellite axes, observed from the inertial frame, are the columns of the three-dimensional square matrix $(\mathsf{T}, -\mathsf{N}, -\mathsf{R})$. Imagine furthermore that there is

TABLE II
THE LIST OF THE ESTIMATED PARAMETERS AT EACH ORBITAL ARC.

Estimated parameters / Satellites	ERS-1	ERS-2	Envisat	TOPEX	Jason-1	Jason-2
Satellite state vector (Cartesian coordinates and velocity components, once per arc)	yes	yes	yes	yes	yes	yes
Atmosphere drag coefficients (times a day)	4–8	4–8	8–10	4	5	5
Along- and cross-track empirical accelerations (once per revolution, times a day)	1–2	1–2	1–2	1	1–2	1–2
SLR range bias (at some stations, once per arc)	yes	yes	yes	yes	yes	yes
A time tag correction for altimeter crossovers relative to SLR data (once per arc)	yes	yes				
DORIS time bias (once per arc)			yes	yes	yes	yes
DORIS station frequency bias (per station, once per pass)			yes	yes	yes	yes
DORIS station troposphere refraction coefficient (per station, per pass)			yes	yes	yes	yes
PRARE station Cartesian coordinates (once per arc)		yes				
PRARE station range bias (per station, once per arc)		yes				
PRARE station time bias (per station, once per arc)		yes				
PRARE station troposphere refraction coefficient (per station, per pass)		yes				
PRARE station 7754 velocities (once per arc)		yes				
Global scaling factor of the solar radiation pressure model (once per arc)				yes	yes	yes

a second person, back-to-back to the first one, endowed with a telescope. That telescope is hinged thus that it can move up and down, but not to the right and to the left. Its operator is supposed to keep the Sun in the crosshair of his instrument all the time.

The restricted mobility of the telescope makes some cooperation between pilot and observer necessary. The pilot must yaw the spacecraft around the axis defined by the line through his head and spine, until the plane in which the telescope can move w.r.t. the vehicle body contains the Sun. This defines the above-mentioned yaw angle Ψ, and the post-multiplication of the matrix $(\mathsf{T}, -\mathsf{N}, -\mathsf{R})$ with the rotation matrix $R_3(-\Psi)$ is the operation that moves the satellite from the nominal orientation to yaw-controlled regime. This achieved, the astronomer pitches his instrument until he sees the Sun.

Now re-interpret the pointing direction of the telescope as the unit vector perpendicular to the solar panels, and you have the situation as it is in a Jason- and TOPEX-like satellite.

Better than a nominal model, however, are attitude data actually measured by a star tracker camera. Such have been obtained both for Jason-1 and for Jason-2. The measured satellite body orientation w.r.t. the inertial reference frame is provided in the form of quaternions, described by a vectorial imaginary part (q_1, q_2, q_3) and a scalar real part q_4, cf. [14, p.5 and p.9]. The attitude matrix derived thereof is

$$M(q) = \begin{pmatrix} 1-2(q_2^2+q_3^2) & 2(q_1q_2-q_3q_4) & 2(q_1q_3+q_2q_4) \\ 2(q_1q_2+q_3q_4) & 1-2(q_1^2+q_3^2) & 2(q_2q_3-q_1q_4) \\ 2(q_1q_3-q_2q_4) & 2(q_2q_3+q_1q_4) & 1-2(q_1^2+q_2^2) \end{pmatrix} \quad (4)$$

where it is understood that

$$\eta_{CIS} = M(q)\,\eta_{SAT} \quad (5)$$

cf. Eq. 1.

Analysis of the attitude data shows that the measured attitude of Jason-1 and Jason-2 is rather close to nominal for most of the duration of each mission, but significantly differs for Jason-1 from 5 July 2012 until the end of the mission, where the yaw steering either was done with the wrong angle, or did not work at all. In this period, the orbit quality of Jason-1 can be expected to benefit from the use of real-world attitude quaternions.

This is clearly seen in Fig. 1–3 showing that applying Jason-1 true attitude reduces the mean values of SLR RMS fits from 2.67 to 1.57 cm, i.e., by 41.1%, DORIS RMS fits from 0.4046 to 0.3561 mm/s, i.e., by 12.0%, two-day orbital arc overlaps from 2.80 to 1.69 cm, i.e., by 39.7%, from 24.40 to 7.27 cm, i.e., by 70.2%, and from 33.57 to 7.95 cm, i.e., by 76.3% in the radial, cross-track and along-track directions, respectively, as compared to the case, when nominal attitude is used at the time interval from 5 July 2012 until 5 July 2013. Still a bit larger observation fits and arc overlaps observed in the last year of the mission (also when using true attitude) are an indication of satellite aging after Jason-1 encountered an anomaly. The Jason-1 orbit quality is rather comparable, when using nominal and true attitude at the time interval from 13 January 2002 until 5 July 2012. Thus, the mean values of SLR RMS fits are 1.26 and 1.24 cm, when using nominal and true attitude, respectively, i.e., they differ by about 1.0%. The mean values of DORIS RMS fits and arc overlaps are comparable, when using nominal and true attitude. A few outliers in the RMS fits and arc overlaps for both curves in Fig. 1–3 are due to the gaps in the observations.

Improvements in the Jason-2 orbit quality, when using true attitude are as follows. The mean values of SLR RMS fits reduce from 1.34 to 1.32 cm, i.e., by 1.0%, DORIS RMS fits improve from 0.3498 to 0.3496 mm/s, i.e., by 0.1%, the two-day orbit arc overlaps in the radial direction improve from 0.85 to 0.84 cm, i.e., by 1.4%.

B. Improvements in satellite macromodels and their impact on orbit quality

Estimation of the global scaling factor of the solar radiation pressure model allowed us to reduce the mean values of SLR RMS fits from 1.63 to 1.38 cm, i.e., by about 15% for Jason-1 and from 1.62 to 1.33 cm, i.e., by about 18% for Jason-2. This gave us an idea, that the macromodels of these satellites and TOPEX/Poseidon used in the EPOS-OC software can be further improved.

Macromodels of TOPEX/Poseidon, Jason-1 and Jason-2 have been improved according to [11]. For all satellites, box-wing macromodels are used. In these models, a satellite is represented by a box with six surfaces and a solar array. For each box surface and the solar array, its area and optical and

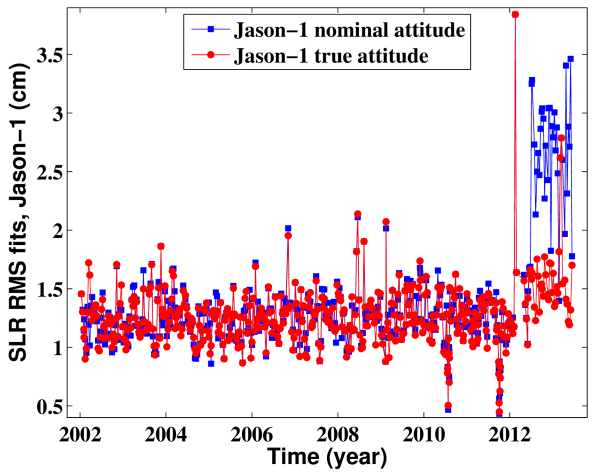

Fig. 1. RMS fits of SLR observations for Jason-1 orbits computed using nominal and true attitude

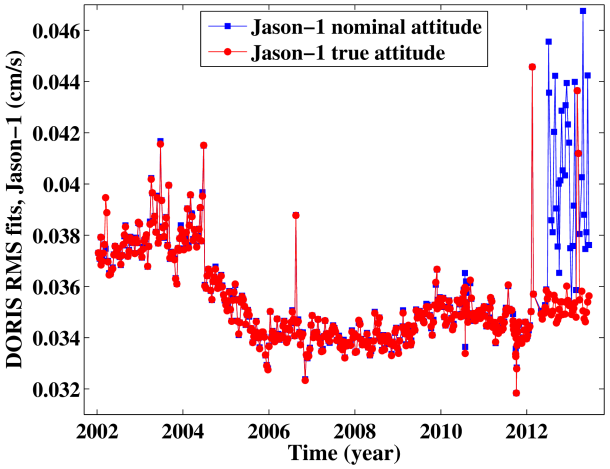

Fig. 2. RMS fits of DORIS observations for Jason-1 orbits computed using nominal and true attitude

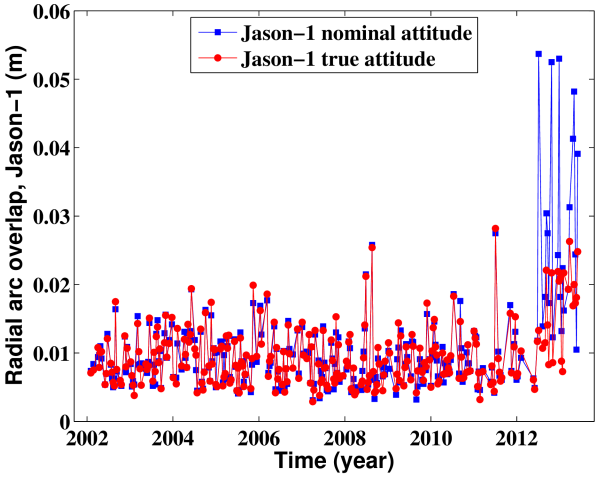

Fig. 3. Two-day arc overlaps in the radial direction for Jason-1 orbits computed using nominal and true attitude

infrared properties given by geometric and diffuse reflection and absorption coefficients are provided together with the orientation of the surfaces and solar array. The improvements include the proper definition of the solar array and optical and infrared properties of the macromodel surfaces.

The improved macromodels reduce SLR RMS fits (Table III) and improve also the internal consistency of the orbits in the radial and cross-track directions provided by the mean value of the two-day arc overlaps in these directions. The internal orbit consistency in the along-track direction slightly deteriorates for TOPEX/Poseidon, but improves for Jason-1 and Jason-2. Larger improvements for Jason-1 and Jason-2 than for TOPEX/Poseidon are explained by the larger average area to mass ratio for Jason-1/2 than for TOPEX/Poseidon: 0.026 and 0.014 m^2/kg, respectively.

C. Impact of tropospheric correction models for DORIS observations on the orbit quality

The uncertainties in the modelling of the path delays due to the troposphere for microwave signals like GPS and DORIS to name a few is the major source of errors in the analysis of these observation types. Hopfield [18] model was applied by [33] to correct DORIS measurements to derive the GFZ VER6 orbits of TOPEX/Poseidon and Envisat. In this study we make use of a tropospheric correction of DORIS measurements based on the Vienna Mapping Functions 1 [8].

The mapping function MF is roughly a function of the inverse of the sinus of the elevation angle E and more precisely using the development in continuous fractions due to [25] can be represented by:

$$MF(E,a,b,c) = \frac{1+\frac{a}{1+\frac{b}{1+c}}}{sinE+\frac{a}{sinE+\frac{b}{sinE+c}}} \quad (6)$$

In the recent years the tropospheric mapping functions have been generated based on operational data from numerical weather models like, e.g., ECMWF ones. The Vienna Mapping Functions 1 are derived from empirical formulae for the b and c coefficients of the continued fraction form, whereas the a coefficients are determined from strict ray-traced mapping functions at 3° elevation.

In the EPOS-OC software the tropospheric correction making use of the VMF1 is implemented according to [20]. The tropospheric slant propagation delay is composed of two parts: the hydrostatic part and the wet part:

$$D = MF_h(E,a_h,b_h,c_h)\cdot z_h + MF_w(E,a_w,b_w,c_w)\cdot z_w \quad (7)$$

where:

D	is total tropospheric slant propagation delay,
MF_h	is hydrostatic mapping function,
MF_w	is wet mapping function,
E	is elevation angle in radians,
a_h, b_h, c_h	are coefficients of the hydrostatic mapping function MF_h,
a_w, b_w, c_w	are coefficients of the wet mapping function MF_w,
z_h	is hydrostatic zenith delay,
z_w	is wet zenith delay.

TABLE III
IMPACT OF THE IMPROVED MACROMODELS ON RMS FITS OF SLR AND DORIS OBSERVATIONS, TWO-DAY ARC OVERLAPS FOR TOPEX/POSEIDON (23 SEPTEMBER 1992 UNTIL 9 OCTOBER 2005), JASON-1 (13 JANUARY 2002 UNTIL 5 JULY 2013) AND JASON-2 (5 JULY 2008 UNTIL 6 APRIL 2015). THE PERCENTAGE OF THE IMPROVEMENT (-) FOR THE NEW MACROMODEL, AS COMPARED TO THE OLD ONE IS SHOWN IN PARENTHESES.

Satellite, macromodel	SLR RMS fits (cm)	DORIS RMS fits (mm/s)	Radial arc overlap (cm)	Cross-track overlap (cm)	Along-track overlap (cm)
TOPEX old	2.02	0.4780	1.03	6.57	3.46
TOPEX new	1.96 (-2.6%)	0.4778 (-0.04%)	0.89 (-13.3%)	6.49 (-1.2%)	3.48 (+0.4%)
Jason-1 old	1.27	0.3538	0.98	4.60	2.64
Jason-1 new	1.19 (-6.9%)	0.3532 (-0.17%)	0.79 (-20.1%)	4.17 (-9.3%)	2.48 (-6.1%)
Jason-2 old	1.32	0.3496	0.84	3.81	1.91
Jason-2 new	1.23 (-7.0%)	0.3490 (-0.17%)	0.56 (-33.5%)	3.34 (-12.2%)	1.46 (-23.8%)

The coefficients for the hydrostatic (a_h) and the wet (a_w) mapping functions as well as the hydrostatic (z_h) and the wet (z_w) zenith delays which are generated by the University of Vienna from ECMWF data at 6-h time interval as a grid with a resolution of 2° in latitude and 2.5° in longitude are bi-linearly interpolated at the location of the observation site.

For a given station location the orography ellipsoidal height is computed by interpolation of a grid file with resolution of 2° in latitude and 2.5° in longitude provided by the University of Vienna. The orography is defined as the average height of land over a certain domain. The higher the horizontal resolution, the better the orography will follow the actual terrain.

The atmospheric pressure is then computed at the orographic ellipsoidal height:

$$P_{oro} = z_h(1 - kcos(2\phi) - 0.28 \cdot 10^{-6} h_{oro})/n \quad (8)$$

where $k = 0.00266$, $n = 0.0022768$.

From the pressure at the orographic height the pressure is then computed at the station height:

$$P_{hsta} = P_{oro} exp(5.225 log(1 - 0.0000226(h_{sta} - h_{oro}))) \quad (9)$$

The hydrostatic zenith delay is evaluated at the station height:

$$z_h(h_{sta}) = nP_{hsta}/(1 - kcos(2\phi) - 0.28 \cdot 10^{-6} h_{sta}) \quad (10)$$

The wet zenith delay at the station height is given by:

$$z_w(h_{sta}) = z_w \cdot exp(-(h_{sta} - h_{oro})/2000) \quad (11)$$

where
h_{sta} is station height,
h_{oro} is orographic ellipsoidal height,
z_w is orographic wet zenith delay,
$z_w(h_{sta})$ is wet zenith delay at station height,
ϕ is station latitude,
P_{oro} is atmospheric pressure at ellipsoidal orographic height,
P_{hsta} is atmospheric pressure at station height.

The major improvement when applying the Vienna Mapping Functions 1 instead of the Hopfield model for the tropospheric correction of DORIS observations is obtained for Envisat. Thus, the mean values of RMS fits reduce by about 2.4% and 2.6% for SLR and DORIS observations, respectively (Table IV, Fig. 4). A jump in DORIS RMS fits is 2004 is due to a change of the procedure of the DORIS data generation. The internal orbit consistency being characterized by the two-day arc overlaps also improve for Envisat by 2.5%, 9.7% and 2.7% in the radial, cross-track and along-track directions, respectively (Table IV). Improvements for Jason-1, when using the VMF1 instead of the Hopfield model, are about 2.0% and 2.6% for SLR and DORIS observations, respectively. The results for Jason-2 are comparable with those for Jason-1. Improvements for TOPEX/Poseidon, when applying the VMF1 instead of the Hopfield model, are about 0.1%, 0.3% for SLR and DORIS observations, respectively. Since the Vienna Mapping Functions 1 are available for the dates since 1 January 1994, global mapping function is used for the dates before this date.

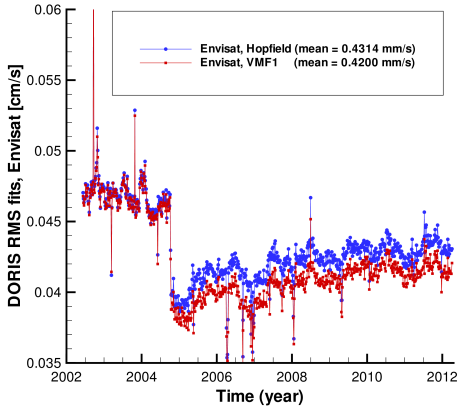

Fig. 4. RMS fits of DORIS observations for Envisat orbits computed using two different tropospheric correction models: the Hopfield model and the Vienna Mapping Functions 1.

III. ORBIT QUALITY ASSESSMENT

A. The main results of precise orbit determination

New precise VER11 orbits of six altimetry satellites have been derived by applying the background models as described by Rudenko et al. (2014) with the updates provided in Section II and Table I. All orbits are computed in the extended ITRF2008 reference frame at the time intervals given in Tables V–VI containing the main results of orbit determination for each satellite. The percentage of the improvement (-) or deterioration (+) of the parameter for the VER11 orbit w.r.t. the VER6 orbit is given in parentheses in these tables. The number of outliers larger than 1 m in the arc overlaps excluded

TABLE IV
IMPACT OF THE HOPFIELD AND VMF1 TROPOSPHERIC CORRECTION MODELS ON RMS FITS OF SLR AND DORIS OBSERVATIONS, TWO-DAY ARC OVERLAPS FOR ENVISAT (OVER 763 ORBITAL ARCS FROM 12 APRIL 2002 UNTIL 8 APRIL 2012). THE PERCENTAGE OF THE IMPROVEMENT (-) FOR THE VMF1, AS COMPARED TO THE HOPFIELD MODEL IS SHOWN IN PARENTHESES.

Model	SLR RMS fits (cm)	DORIS RMS fits (mm/s)	Radial arc overlap (cm)	Cross-track overlap (cm)	Along-track overlap (cm)
Hopfield	1.30	0.4314	0.52	2.09	2.16
VMF1	1.27 (-2.4%)	0.4200 (-2.6%)	0.51 (-2.5%)	1.89 (-9.7%)	2.10 (-2.7%)

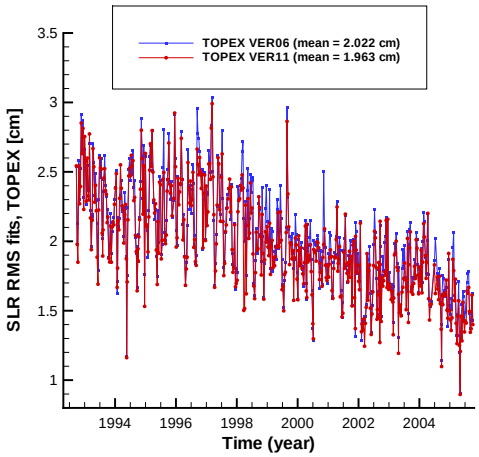

Fig. 5. RMS fits of SLR observations for the GFZ VER6 and VER11 orbits of TOPEX/Poseidon.

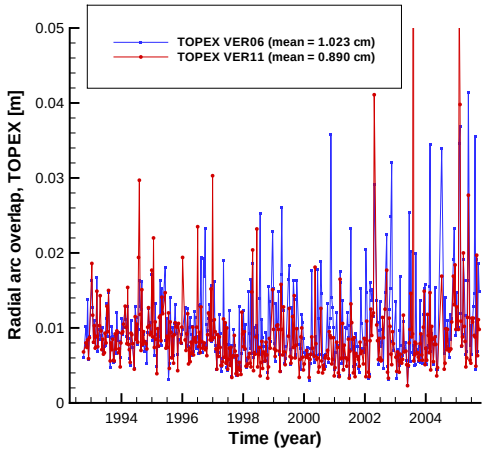

Fig. 6. Two-day arc overlaps in radial direction for the GFZ VER6 and VER11 orbits of TOPEX/Poseidon.

for both VER6 and VER11 orbit solutions is 54 for ERS-1, 16 for ERS-2 and 14 for Jason-1. Most outliers occur at the arcs either with gaps in observations or when satellite attitude does not follow the nominal attitude.

The new VER11 orbits show improvements w.r.t. previous VER6 orbits. Significant orbit quality improvements have been obtained for Jason-1, Jason-2, TOPEX/Poseidon and Envisat. The orbit quality of ERS-1 and ERS-2 also improve. Figures 5–6 show the improvements in the RMS fits of SLR observations and two-day arc overlaps in the radial direction for the GFZ VER11 orbit, as compared to the GFZ VER6 orbit of TOPEX/Poseidon.

B. Orbit quality assessment by single-satellite crossover analysis

A single-satellite altimetry crossover analysis of the GFZ VER11 orbits has been performed applying the procedure described by [36]. The mean values of RMS and mean of the crossover differences for the GFZ VER11, VER6 and selected external orbits derived at Goddard Space Flight Center (GSFC), Centre National d'Etudes Spatiales (CNES), European Space Operations Centre (ESOC) of the European Space Agency (ESA), within REAPER ('Reprocessing of Altimeter Products for ERS') project [32] and available from AVISO CNES data center[2] are given in Table VII. ESOC V.08 orbits were computed using the procedures described by [15] with updates described at ftp://dgn6.esoc.esa.int/envisat/sol8/envisat.sol8.txt. For all TOPEX/Poseidon orbits, altimeter data only from one – TOPEX – altimeter were used.

Our analysis shows that the GFZ VER11 orbits give smaller mean value of the RMS of the crossover differences, as compared to the GFZ VER6 orbits for all six satellites, namely, by 0.05, 0.02, 0.79, 0.07, 0.17 and 0.19 cm for ERS-1, ERS-2, Envisat, TOPEX/Poseidon, Jason-1, and Jason-2, respectively. Figures 7 and 8 show significant improvement in the RMS and mean of the crossover differences for the GFZ VER11 orbit, as compared to the GFZ VER6 orbit for TOPEX/Poseidon. The mean values of RMS of the crossover differences of the GFZ VER11 orbits show better (smaller) values, as compared to the external orbit solutions, by 5.5% for ERS-1, 1.4% for ERS-2 and 13.6–14.5% for Envisat, and are slightly worse for TOPEX/Poseidon (by 1.0%), Jason-1 (by 2.0%) and Jason-2 (by 0.8%).

C. Orbit quality assessment by multi-mission crossover analysis

Since single-satellite crossover analysis is not able to provide information on the geographical pattern of mean radial errors in altimetry measurements (which are typical for remaining uncertainties of POD), a multi-mission crossover analysis is performed. This method can also be applied to extract information on the inter-mission consistency of the data sets. The approach used here is based on all past and current altimetry missions. Thus, in addition to ERS-1, ERS-2, Envisat, TOPEX, Jason-1, and Jason-2, data from GFO, Cryosat-2,

[2]http://www.aviso.altimetry.fr/en/home.html

TABLE V
THE MEAN VALUES OF RMS FITS OF OBSERVATIONS, TWO-DAY ARC OVERLAPS AND THE NUMBER OF ARCS USED TO COMPUTE THESE VALUES FOR THE ERS-1 (1 AUGUST 1992 UNTIL 5 JULY 1996) AND ERS-2 (13 MAY 1995 UNTIL 28 FEBRUARY 2006) VER6 AND VER11 ORBITS COMPUTED AT THE TIME INTERVALS GIVEN IN PARENTHESES.

Satellite and orbit version	SLR RMS fits (cm)	SXO RMS fits (cm)	PRARE range RMS fits (cm)	PRARE Doppler RMS fits (mm/s)	Radial arc overlap (cm)	Cross-track overlap (cm)	Along-track overlap (cm)	Number of arcs SLR/SXO/PRA/Ov.
ERS-1 VER6	2.15	4.79	—	—	1.84	17.14	12.14	373/361/—-/228
ERS-1 VER11	2.13 (-0.9%)	4.77 (-0.3%)	—	—	1.82 (-0.7%)	16.46 (-4.0%)	12.09 (-0.4%)	373/361/—-/228
ERS-2 VER6	1.70	4.10	3.46	0.3931	1.84	7.11	10.69	793/779/258/580
ERS-2 VER11	1.69 (-0.2%)	4.11 (+0.2%)	3.48 (+0.6%)	0.3947 (+0.4%)	1.85 (+0.9%)	7.24 (+1.8%)	10.63 (-0.5%)	793/779/258/580

TABLE VI
THE MEAN VALUES OF RMS FITS OF SLR AND DORIS OBSERVATIONS, TWO-DAY ARC OVERLAPS AND THE NUMBER OF ARCS USED TO COMPUTE THESE VALUES FOR TOPEX/POSEIDON (23 SEPTEMBER 1992 UNTIL 9 OCTOBER 2005), ENVISAT (12 APRIL 2002 UNTIL 8 APRIL 2012), JASON-1 (13 JANUARY 2002 UNTIL 5 JULY 2013), AND JASON-2 (5 JULY 2008 UNTIL 6 APRIL 2015) VER6 AND VER11 ORBITS COMPUTED AT THE TIME INTERVALS GIVEN IN PARENTHESES.

Satellite and orbit version	SLR RMS fits (cm)	DORIS RMS fits (mm/s)	Radial arc overlap (cm)	Cross-track overlap (cm)	Along-track overlap (cm)	Number of arcs SLR/DORIS/Overlap
TOPEX VER6	2.02	0.4797	1.02	6.53	3.59	494 / 459 / 433
TOPEX VER11	1.96 (-2.9%)	0.4778 (-0.4%)	0.89 (-12.8%)	6.49 (-0.6%)	3.48 (-3.2%)	494 / 459 / 433
Envisat VER6	1.30	0.4314	0.52	2.09	2.16	763 / 749 / 594
Envisat VER11	1.27 (-2.3%)	0.4214 (-2.3%)	0.53 (+3.1%)	1.98 (-5.3%)	1.93 (-10.4%)	763 / 760 / 594
Jason-1 VER6	1.63	0.3641	0.95	5.96	4.52	443 / 443 / 274
Jason-1 VER11	1.19 (-27.3%)	0.3532 (-3.0%)	0.79 (-17.0%)	4.17 (-30.0%)	2.48 (-45.1%)	441 / 441 / 270
Jason-2 VER6	1.62	0.3510	0.82	4.04	3.94	255 / 251 / 192
Jason-2 VER11	1.23 (-24.3%)	0.3490 (-0.6%)	0.56 (-31.8%)	3.34 (-17.2%)	1.46 (-63.1%)	255 / 251 / 190

TABLE VII
THE MEAN VALUES OF RMS AND MEAN OF THE CROSSOVER DIFFERENCES FOR GFZ AND EXTERNAL ORBITS FOR EACH SATELLITE COMPUTED AT THE FOLLOWING TIME INTERVALS: 9 JULY 1992 TO 30 MAY 1996 FOR ERS-1, 15 MAY 1995 TO 16 JUNE 2003 FOR ERS-2, 21 MAY 2002 TO 3 APRIL 2012 FOR ENVISAT, 9 APRIL 1993 TO 30 SEPTEMBER 2005 FOR TOPEX/POSEIDON, 15 JANUARY 2002 TO 13 JANUARY 2012 FOR JASON-1, AND 4 JULY 2008 TO 3 APRIL 2015 FOR JASON-2. THE BEST VALUES FOR EACH SATELLITE ARE MARKED IN BOLD.

Orbit solution	Crossover RMS (cm)	Crossover mean (cm)
ERS-1 REAPER combined	6.32	0.22
ERS-1 GFZ VER6	6.02	0.24
ERS-1 GFZ VER11	**5.97**	**0.11**
ERS-2 REAPER combined	6.41	**-0.01**
ERS-2 GFZ VER6	6.34	0.04
ERS-2 GFZ VER11	**6.32**	0.01
Envisat AVISO GDR-C	5.94	0.32
Envisat ESOC V.08	6.00	**0.24**
Envisat GFZ VER6	5.92	0.44
Envisat GFZ VER11	**5.13**	0.60
TOPEX/Poseidon CNES GDR-C	5.40	-0.37
TOPEX/Poseidon GSFC std1204	**5.21**	**-0.18**
TOPEX/Poseidon GFZ VER6	5.33	**-0.18**
TOPEX/Poseidon GFZ VER11	5.26	-0.26
Jason-1 CNES GDR-C	5.04	0.35
Jason-1 CNES GDR-D	**4.93**	**0.05**
Jason-1 GFZ VER6	5.20	0.40
Jason-1 GFZ VER11	5.03	0.47
Jason-2 CNES GDR-D	**4.93**	**0.10**
Jason-2 GFZ VER6	5.16	0.23
Jason-2 GFZ VER11	4.97	0.33

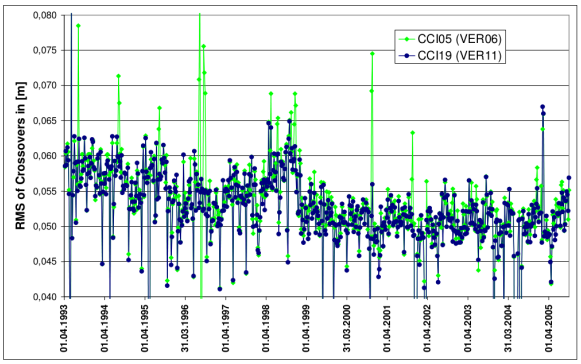

Fig. 7. RMS of the crossover differences of the GFZ TOPEX/Poseidon VER6 and VER11 orbits.

ICESat, and Saral are included in the analysis. In order to ensure a harmonized data set, identical correction models are applied to the data whenever possible (e.g., for tides and the dynamic atmospheric correction). Then, sea surface height crossover differences are computed and minimized in an adjustment process in order to estimate time series of radial errors for all missions involved in the process. By analysing the estimated radial errors (e.g., performing frequency analysis or computation of geographically correlated mean errors) information on the quality and consistency of the single satellite data sets are derived. However, it has to be kept in mind that radial orbit errors are only one part of the radial errors – but probably the most significant part. Moreover, comparing the solutions computed based on different orbits will give information on the accuracy differences of the orbit solutions. A detailed description of the method is given in [9]. The software parameters as well as the altimeter data sets described there are exactly the same as used in this study – except for the orbits which are replaced by GFZ orbits for all missions under investigation. In order to allow for comparisons with external results, the crossover analysis is also performed based on external orbits, namely GSFC std0809 orbit [4] for TOPEX,

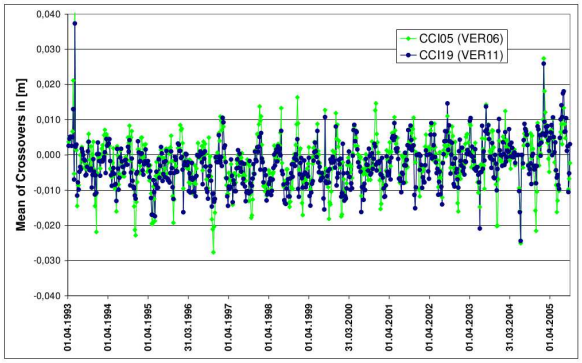

Fig. 8. Mean of the crossover differences of the GFZ TOPEX/Poseidon VER6 and VER11 orbits.

TABLE VIII
STANDARD DEVIATIONS AND MEANS (IN PARENTHESES) OF RADIAL ERRORS FOR EACH MISSION AND DIFFERENT ORBIT SOLUTIONS IN [CM].

Satellite	GFZ VER11	GFZ VER6	external
ERS-1	1.75 (44.34)	1.84 (44.32)	1.87 (44.15)
ERS-2	2.51 (7.09)	2.53 (7.13)	2.36 (6.93)
Envisat	1.74 (44.89)	1.74 (45.05)	1.78 (45.07)
TOPEX	1.49 (-0.06)	1.59 (-0.00)	1.45 (-0.00)
Jason-1	1.55 (9.71)	1.77 (9.62)	1.25 (9.87)
Jason-2	1.10 (-0.52)	1.39 (-0.52)	1.08 (-0.52)

REAPER combined orbits [32] for ERS-1 and ERS-2, and GDR-D orbits for Envisat (ESA[3]), Jason-1 (CNES[4]), and Jason-2 (AVISO[5]).

1) Scatter and frequencies of radial errors: The scatters of radial errors provide information on the precision and consistency of the different data sets. Table VIII shows the standard deviations of the time series for all missions. These values include noise as well as systematic errors. The latter part will be analysed in more detail later. For all missions the newer GFZ orbit version (VER11) performs better or equal than the older one (VER6). The improvements are larger for the NASA/CNES missions (TOPEX and Jason) than for the ESA missions (ERS and Envisat). With respect to the external orbit solutions, one can see a better performance for the GFZ orbit VER11 for ERS-1 and Envisat and similar or worse performance for the other missions. The means of radial errors differ significantly between the missions. However, they are not interpreted in detail here since they represent inter-mission offsets and are mostly due to instrumental offsets of the altimeter systems and not due to orbit uncertainties. The changes due to different orbits are mostly below 2 mm as visible from Table VIII.

In order to analyse the behaviour of radial errors in more detail, a frequency analysis is performed for each time series in order to define the dominant periods and their amplitudes. It shows that for most missions the most prominent period

[3]ftp://diss-nas-fp.eo.esa.int/doris/vor_gdr_d
[4]ftp://cddis.gsfc.nasa.gov/pub/doris/products/orbits/ssa/ja1
[5]ftp://avisoftp.cnes.fr/AVISO/pub/jason-2

TABLE IX
RESULT OF SPECTRAL ANALYSIS OF RADIAL ERRORS: AMPLITUDES FOR ORBIT REVOLUTION PERIOD IN [MM]. NOTE: WITHOUT GEODETIC MISSION PHASE FOR THE GFZ VER6 JASON-1 ORBIT.

Satellite	GFZ VER11	GFZ VER6	external
ERS-1	1.4	1.3	1.2
ERS-2	12.0	10.0	7.2
Envisat	6.0	5.0	3.0
TOPEX	1.4	3.0	1.5
Jason-1	2.3	3.9	1.2
Jason-2	1.3	3.9	1.3

is given by the orbit revolution frequency (1/rev) indicating some possible remaining problems with the modelling of non-gravitational forces and the satellite macromodels. The amplitudes for these periods are given in Table IX for all missions. For the NASA/CNES missions the results clearly improve from VER6 to VER11. This is mainly due to the improvements in the satellite macromodels and attitude modelling for these missions. The VER6 orbit quality for the geodetic phase of Jason-1 (2012/2013) was significantly degraded (amplitude of 20.3 cm) and was excluded from the analysis. For the ESA missions (slightly) decreasing precision is visible from VER6 to VER11. Compared to external orbit solutions there is still room for improvement, especially for ERS-2 and Envisat but also for Jason-1. For TOPEX and Jason-2, the GFZ VER11 orbit behaves similar or better than external orbit products. The amplitudes themselves also depend on the measurement period of the missions, e.g., for ERS-2 the amplitude is highest due to the extreme solar activity between 2000 and 2002.

2) Geographically correlated mean errors: Supplementary to the temporal behaviour the spatial behaviour of radial errors is interesting and is analysed in more detail. For this purpose, the radial errors of each mission are separated in ascending and descending passes and averaged within $3^\circ \times 3^\circ$ geographic cells. These grids can be used to derive information on the differences between ascending and descending passes (see section III-B) as well as on geographically correlated mean errors (GCE). The latter ones are built by averaging the ascending value and the descending value per grid cell to derive a mean. This quantity will not cancel out when using all satellite passes and will therefore directly map in the sea surface height estimation. More information on the method to estimate GCE is available in [9] and [12].

Figure 9 shows GCE for all missions computed with the GFZ VER11 orbit (left) and external orbits (middle) as well as the differences between both solutions (right). For all missions, large scale patterns with amplitudes up to about 1 cm are visible. At least for 94% of the area, differences smaller than 5 mm are reached. The patterns are similar for both orbit versions and also the standard deviations (Table X) show only small differences. For ERS-2, TOPEX, and Jason-2, the VER11 orbits behave better than the external orbits. For the other three missions the results are similar or slightly worse with VER11. The remaining differences have zero mean and reach up to 3.5 mm standard deviations (ERS-2). For ERS-2, 72% of the differences are smaller than 1 mm. These percentages increase for the other missions up to 90% (for TOPEX and Envisat). Since the whole time series are used to compute one set of

TABLE X
STANDARD DEVIATION OF GEOGRAPHICALLY CORRELATED ERRORS IN [MM].

Satellite	GFZ VER11	GFZ VER6	external
ERS-1	2.64	2.62	2.63
ERS-2	3.46	3.38	3.77
Envisat	2.98	2.89	2.72
TOPEX	1.90	2.01	2.06
Jason-1	1.70	2.23	1.63
Jason-2	1.58	1.80	1.72

GCE per mission, no information on the temporal behaviour is included in these results. This is necessary in order to employ enough data to extract reliable results. However, variations of the GCE pattern over time might occur, e.g., due to drifts in the realization of the reference frame.

While for TOPEX and Jason-1/2 VER11 behaves better than the older GFZ orbit versions, for ESA missions (ERS-1/2 and Envisat) VER6 seems to be of better quality than VER11. This is visible in the temporal as well as in the spatial analysis of the estimated radial errors. The quality of GFZ orbits is of the same order of magnitude as other external orbit solutions. However, for most missions some challenges regarding the modelling of non-gravitational forces still remain. This holds especially for Jason-1 and the ESA missions. On the other hand, the geographically correlated errors which are especially harmful for precise sea level estimations are smaller by about 8% in the GFZ VER11 version than for external orbit versions for three missions (ERS-2, TOPEX, and Jason-2).

D. Orbit quality assessment based on sea level anomalies

To assess the impact of the orbit versions on sea level variability we perform collinear analyses for the Envisat, TOPEX, Jason-1 and Jason-2 missions considering three orbit solutions for each mission, i.e., VER6 and VER11 orbits and a reference orbit (REF). Based on the previous analysis we have chosen the following reference orbits: GSFC std1204 [21] for TOPEX, ESOC V.08 for Envisat, CNES GDR-D for Jason-1 and AVISO GDR-D for Jason-2. The periods considered are 4/1993–10/2005 for TOPEX, 6/2002–10/2010 for Envisat, 1/2002–12/2011 for Jason-1 and 7/2008–12/2014 for Jason-2.

The along-track sea level anomalies are interpolated to monthly $1^\circ \times 1^\circ$ grids and monthly time series of global mean RMS (GRMS) of the sea level differences for VER6, VER11 and REF orbits are derived. In the following we assume that a decrease in the global mean sea level variability indicates a prevalence of the corresponding orbit. The temporal mean of the GRMS values is given in Table XI. The time series of GRMS differences for VER11–VER6 and VER11–REF are shown in Fig. 10 for all four missions.

The differences of the mean GRMS values (Table XI) are predominantly smaller than 0.02 cm. The VER11 series outperforms the VER6 series for Jason-1 and Jason-2. For Envisat, the performance of VER11 and VER6 orbits is almost identical. However, for TOPEX, the VER11 orbit is slightly degraded with respect to the VER6 orbit. Further analyses of the TOPEX global mean RMS differences show (Fig. 10) that

TABLE XI
MEAN GLOBAL ($\pm 60^\circ$) RMS OF SEA LEVEL IN CM FROM MONTHLY GRIDDED DATA FOR FOUR MISSIONS AND ALL AVAILABLE COLLINEAR DATA FOR TWO GFZ ORBITS AND THE REFERENCE ORBITS (GSFC STD1204, ESOC, CNES, AVISO). MINIMUM VALUES ARE MARKED BOLD FOR EACH MISSION.

Orbit	TOPEX (4/1993–10/2005)	Envisat (6/2002–10/2010)	Jason-1 (1/2002–12/2011)	Jason-2 (7/2008–12/2014)
GFZ VER6	**5.62**	**6.49**	5.38	5.38
GFZ VER11	5.64	**6.49**	**5.37**	5.34
REF	5.63	6.52	**5.37**	**5.32**

the degradation of the VER11 orbit w.r.t. the VER6 orbit takes place from 1999 to mid of 2002. During this period the RMS differences are governed by a pronounced annual signal.

The GFZ VER11 orbit exhibit smaller mean GRMS values than the corresponding reference orbit for Envisat. For TOPEX and Jason-1, the performance of the GFZ VER11 orbits is almost identical to that one of the REF orbits, while for Jason-2 the REF orbit is slightly better. A striking feature of the Jason GRMS difference series w.r.t. to those of the REF orbits are recurrent annual signals (Fig. 10). These signals are exceptionally strong for Jason-2 and imply a better performance of the REF orbits during summer/autumn while the VER11 orbits perform better during winter/spring.

IV. IMPACT OF ORBIT CHOICE ON GLOBAL AND REGIONAL SEA LEVEL TRENDS

The global mean sea level trend estimated from altimetry is impacted by the choice of the orbit model. Important factors are, among others, the stability of the reference system and the details of the time variable gravity field model used [33]. To assess this impact we have calculated monthly global mean sea level (GMSL) and estimated global and regional trends based on the $1^\circ \times 1^\circ$ grids of sea level anomalies of the TOPEX, Jason-1, Jason-2 series. The mean sea level curves, GMSL trends and the differences of the GMSL trends estimated based on the VER6, VER11 and REF orbits are given in Fig. 11. In general, the GMSL differences between the different orbits are of the order of 5 mm to maximum 10 mm and rather high-frequent. For TOPEX, the agreement between the GMSL series based on VER11 and REF orbits is higher than for the ones based on VER6 and VER11 orbits. The global mean sea level trend for the period 03/1993 to 12/2014 is 2.8, 3.0, and 3.1 mm/year based on the VER6, VER11 and REF orbits, respectively. The observed differences in decadal global mean sea level trend are well below the uncertainty of the state-of-the art SL_cci altimetry product of 0.5 mm/year [1]. However, since we exchange the orbit solutions only and the formal error of the fit is of the order of 0.04 mm/year we consider the observed changes in the GMSL trend as significant. The improvements described in Section II result in a shift (bias) of about 3 mm of the GMSL of VER11 orbits w.r.t. the GMSL of VER6 orbits starting from autumn 1998. In addition, for the Jason-2 mission the GMSL difference from the GFZ and the reference (AVISO GDR-D) orbits is drifting in the order of 0.6 mm/year.

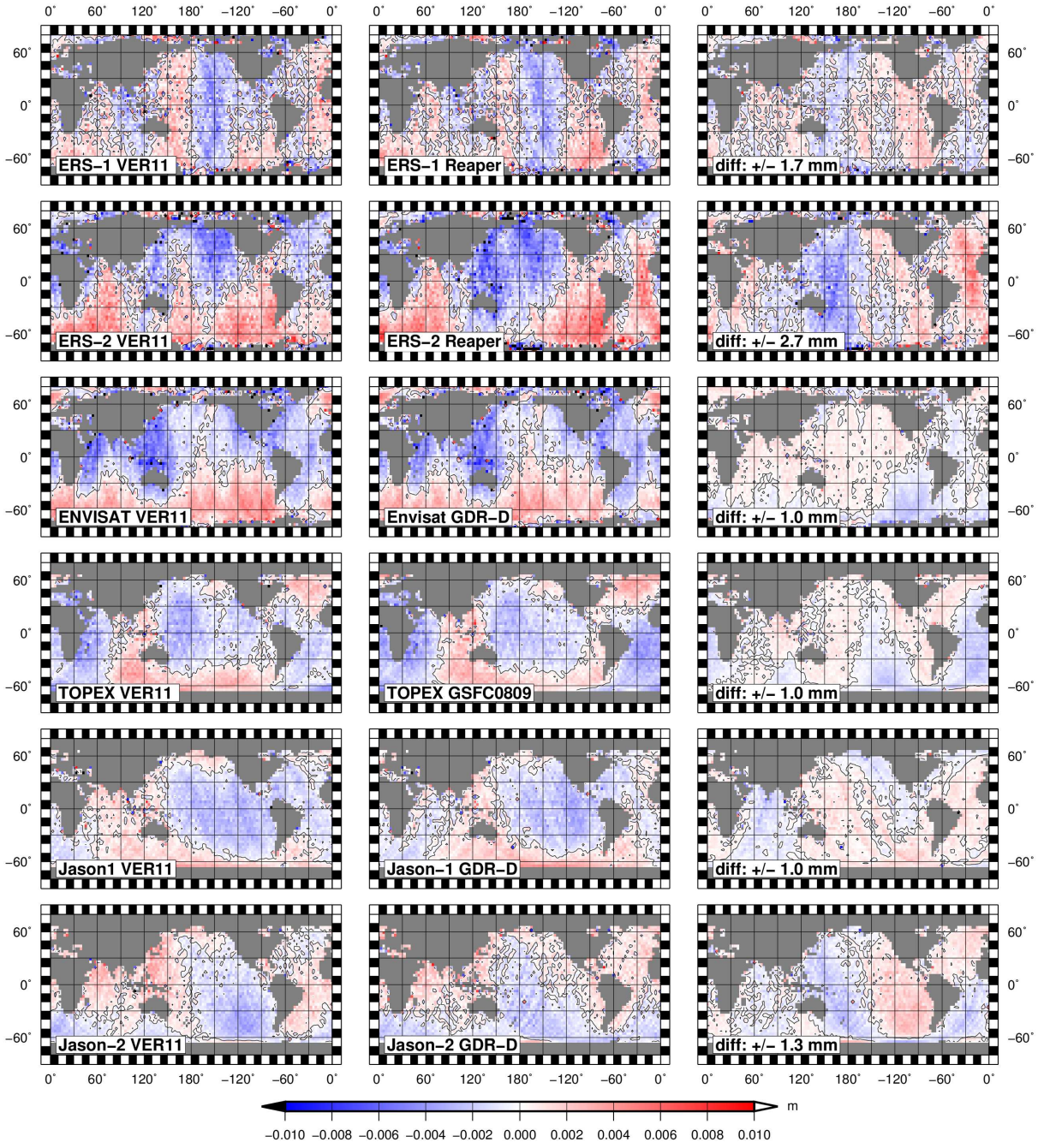

Fig. 9. Geographically correlated errors based on the GFZ VER11 orbits for all six missions (left) and based on external orbits (middle). The right column displays the differences between the two orbit solutions.

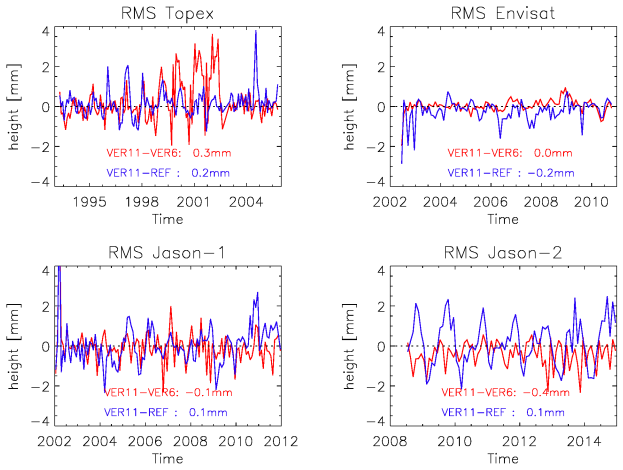

Fig. 10. Monthly differences of the global mean (±60°) RMS of sea level anomalies based on the VER6, VER11 and REF orbits for TOPEX, Envisat, Jason-1 and Jason-2. Negative values imply superior performance of the VER11 orbits. The temporal mean difference of the RMS values is given at the lower part of the figures.

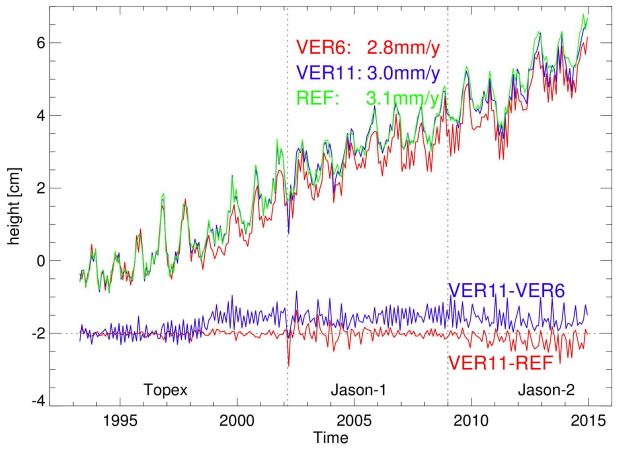

Fig. 11. Global mean sea level (±60°) based on the VER6 (red), VER11 (blue) and REF (green) orbits. The GMSL differences for the VER11–VER6 (blue) and the VER11–REF (red) series are shown at the bottom shifted by an arbitrary number.

The regional sea level trends based on the VER11 orbits and the differences of the trends based on the VER11 and REF orbits are shown in Fig. 12 for the period 04/1993–12/2014 from TOPEX, Jason-1 and Jason-2. The differences related to the choice of orbit are mainly in the order of 1 mm/year, which corresponds to up to 50% of the mean regional value in eastern South Pacific. Further analyses show that the regional trend differences are dominated by Jason-1.

V. Conclusion

Using the new background models for precise orbit determination we have obtained the following improvements. The improved macromodels reduce the SLR RMS fits by 2.6%, 6.9% and 7.0% for TOPEX/Poseidon, Jason-1, and Jason-2, respectively. The internal consistency of the orbits also improves. Thus, radial arc overlaps improve by 13.3%,

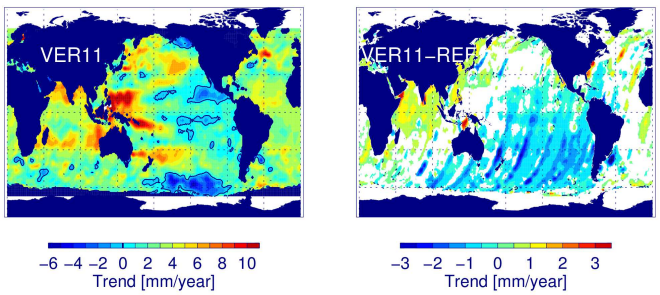

Fig. 12. Sea level trend for the period 04/1993–12/2014 from TOPEX, Jason-1 and Jason-2 based on the VER11 orbits (left) and trend difference based on the VER11 and REF-orbits (right). Regions where the differences are less than 10% of the total trends are marked out (white). The zero-contour is sketched.

20.1%, and 33.5% for these satellites, respectively. Applying true attitude instead of models brings an improvement of SLR RMS by 1% for Jason-1 and Jason-2 for the most of the duration of each mission and up to 41% for Jason-1 at the time span from 5 July 2012 until 5 July 2013, when the satellite did not follow the nominal attitude. Applying the Vienna Mapping Functions 1 instead of the Hopfield model for the tropospheric correction of DORIS observations reduces the mean values of SLR observations by about 2.0–2.4% and those of DORIS observations by 2.6% for Envisat and Jason satellites. Two-day arc overlaps improve at the same time for Envisat by 2.5%, 9.7% and 2.7% in the radial, cross-track and along-track directions, respectively.

At the same time, using the EIGEN-6S4 geopotential model instead of the EIGEN-6S2 geopotential model has minor impact on the SLR RMS fits. They increase by 0.2–0.3% for ERS-2, Envisat, TOPEX/Poseidon, Jason-1, Jason-2 and decrease by 0.3% for ERS-1. Applying the EOT11a ocean tide model instead of the EOT10a model has also minor impact on SLR residuals. They increase by 0.04% for ERS-1 and 0.19% for ERS-2, do not change for TOPEX/Poseidon, and decrease by 0.14% for Envisat and 0.04% for Jason-1. Based on the results of these tests, an optimum set of the background models for orbit determination has been defined.

Using this set of updated background models in the extended ITRF2008 reference frame new, precise and consistent VER11 orbits have been derived at GFZ German Research Centre for Geosciences for six altimetry missions. They comprise the altimetry satellites ERS-1 (1 August 1991 – 5 July 1996), ERS-2 (13 May 1995 – 27 February 2006), TOPEX/Poseidon (23 September 1992 – 8 October 2005), Envisat (12 April 2002 – 8 April 2012), Jason-1 (13 January 2002 – 5 July 2013) and Jason-2 (5 July 2008 – 5 April 2015) and in total cover a 23-year time span (1991–2015). The mean values of the SLR RMS fits are 2.13, 1.69, 1.27, 1.96, 1.19 and 1.23 cm for ERS-1, ERS-2, Envisat, TOPEX/Poseidon, Jason-1 and Jason-2 satellites, respectively, for the GFZ VER11 orbits. The mean values of the DORIS RMS fits are 0.4778, 0.4214, 0.3532 and 0.3490 mm/s for the new orbits of TOPEX/Poseidon, Envisat, Jason-1 and Jason-2, respectively. The internal orbit consistency of new orbits in the radial direction is 1.82, 1.85, 0.53, 0.89, 0.79, and 0.56 cm for ERS-1, ERS-2, Envisat, TOPEX/Poseidon,

Jason-1 and Jason-2, respectively. The internal orbit consistency of the new orbits in the cross-track direction is 16.46, 7.24, 1.98, 6.49, 4.17, and 3.34 cm for ERS-1, ERS-2, Envisat, TOPEX/Poseidon, Jason-1 and Jason-2, respectively. Finally, the internal orbit consistency of the new orbits in the along-track direction is 12.09, 10.63, 1.93, 3.48, 2.48, and 1.46 cm for ERS-1, ERS-2, Envisat, TOPEX/Poseidon, Jason-1 and Jason-2, respectively.

Single-satellite altimetry crossover analysis indicates reduction (improvement) of the mean values of RMS of the single-satellite altimetry crossover differences computed using the GFZ VER11 orbits, as compared to the GFZ VER6 orbits by 0.05, 0.02, 0.79, 0.07, 0.17 and 0.19 cm for ERS-1, ERS-2, Envisat, TOPEX/Poseidon, Jason-1, and Jason-2, respectively. The mean value of the RMS of the crossover differences computed using the GFZ VER11 orbits is 5.97, 6.32, 5.13, 5.26, 5.03, and 4.97 cm for ERS-1, ERS-2, Envisat, TOPEX/Poseidon, Jason-1 and Jason-2, respectively.

The multi-mission altimetry crossover analysis gives the following standard deviation of radial errors for the GFZ VER11 orbits: 1.75, 2.51, 1.74, 1.49, 1.55, and 1.10 cm for ERS-1, ERS-2, Envisat, TOPEX/Poseidon, Jason-1 and Jason-2, respectively. This shows reduction of the standard deviation of radial errors of the GFZ VER11 orbits of all missions, as compared to the GFZ VER6 orbits. The temporal as well as the spatial analysis of the estimated radial errors indicates that for TOPEX and Jason-1/2, VER11 orbits behave better than the older GFZ orbit versions, while for ESA missions (ERS-1/2 and Envisat), VER6 orbits seem to be of better quality than VER11 orbits. On the other hand, the geographically correlated errors which are especially harmful for precise sea level estimations are smaller by about 8% in the GFZ VER11 version than for external orbit versions for three missions (ERS-2, TOPEX, and Jason-2). However, for most missions some challenges regarding the modelling of non-gravitational forces remain. This holds especially for Jason-1 and the ESA missions.

The global mean sea level trend for the period 03/1993 to 12/2014 based on TOPEX, Jason-1 and Jason-2 altimeter data is varying by 0.3 mm/year (2.8 to 3.1 mm/year) depending on the orbit selection. The GMSL trend has risen by 0.2 mm/year to 3.0 mm/year from the GFZ VER6 to VER11 orbit and is dominated by changes in the TOPEX orbit starting in autumn 1998. The GMSL trend from the GFZ VER11 orbits is lower by 0.1 mm/year w.r.t. that one from the reference orbits which is related to differences in the Jason-2 orbits. Regionally, the trends from the reference and the GFZ VER11 altimeter series differ in the order of 1 mm/year with maxima in the eastern South Pacific and the northern Indian Ocean. The trend differences reach up to 50% of the mean regional values in eastern South Pacific and mainly originate from Jason-1 orbits.

Based on the results of our study we recommend the GFZ VER11 orbits for applications requiring precise orbits of all six satellites in question derived in the same reference frame using consistent background models for orbit determination. Even though significant improvements have been obtained at GFZ for the VER11 orbits of TOPEX/Poseidon, Jason-1 and Jason-2, as compared to the VER6 ones, the enhancement of satellite-specific models as well as modelling of non-gravitational forces used in the EPOS-OC software should further increase the orbit quality for these missions.

VI. Data availability

The GFZ VER11 orbits of altimetry satellites are available via anonymous ftp. The description on the access is given in the file ftp://ftp.gfz-potsdam.de/pub/home/kg/orbit/SLCCI/Readme_GFZ_VER11_SLCCI_orbits.

References

[1] M. Ablain, A. Cazenave, G. Larnicol, M. Balmaseda, P. Cipollini, Y. Faugere, M. J. Fernandes, O. Henry, J. A. Johannessen, P. Knudsen, O. Andersen, J. Legeais, B. Meyssignac, N. Picot, M. Roca, S. Rudenko, M. G. Scharffenberg, D. Stammer, G. Timms, J. Benveniste, "Improved sea level record over the satellite altimetry era (1993–2010) from the Climate Change Initiative project," *Ocean Sci.*, vol. 11, pp. 67-82, 2015.

[2] Z. Altamimi, X. Collilieux, J. Legrand, B. Garayt, C. Boucher, "ITRF2005: A new release of the International Terrestrial Reference Frame based on time series of station positions and Earth Orientation Parameters," *J. Geophys. Res.*, vol. 112, no. B9, B09401, 2007.

[3] Z. Altamimi, X. Collilieux, L. Métivier, "ITRF2008: an improved solution of the international terrestrial reference frame," *J. Geod.*, vol. 85, pp. 457–473, 2011.

[4] B. D. Beckley, F. G. Lemoine, S. B. Luthcke, R. D. Ray, N. P. Zelensky, "A reassessment of global and regional mean sea level trends from TOPEX and Jason-1 altimetry based on revised reference frame and orbits," *Geophys. Res. Lett.*, vol. 34, L14608, 2007.

[5] R. Biancale, A. Bode, "Mean annual and seasonal atmospheric tide models based on 3-hourly and 6-hourly ECMWF surface pressure data," GFZ Scientific Technical Report 06/01, doi:10.2312/GFZ.b103-06011, 2006.

[6] J. Boehm, A. E. Niell, P. Tregoning, H. Schuh, "Global Mapping Functions (GMF): a new empirical mapping function based on numerical weather model data," *Geophys. Res. Lett.*, vol. 33, L07304, 2006.

[7] J. Boehm, R. Heinkelmann, H. Schuh, "Short Note: a global model of pressure and temperature for geodetic applications," *J. Geod.*, vol. 81, pp. 679–683, 2007.

[8] J. Boehm and H. Schuh, "Vienna mapping functions in VLBI analyses," *Geophys. Res. Lett.*, vol. 31, L01603, 2004.

[9] W. Bosch, D. Dettmering, C. Schwatke, "Multi-mission cross-calibration of satellite altimeters: constructing a long-term data record for global and regional sea level change studies," *Remote Sensing*, vol. 6, no. 3, pp. 2255–2281, 2014.

[10] L. Cerri, J. P. Berthias, W. I. Bertiger, B. J. Haines, F. G. Lemoine, F. Mercier, J. C. Ries, P. Willis, N. P. Zelensky, M. Ziebart, "Precision orbit determination standards for the Jason series of altimeter missions," *Mar. Geod.*, vol. 33, no. S1, pp. 379–418, 2010.

[11] L. Cerri and P. Ferrage, "DORIS satellites model implemented in POE processing," Ed.1, Rev. 7. SALP-NT-BORD-OP-16137-CN, CNES, 2014. ftp://ftp.ids-doris.org/pub/ids/satellites/DORISSatelliteModels.pdf

[12] D. Dettmering and W. Bosch, "Global calibration of Jason-2 by multi-mission crossover analysis," *Mar. Geod.*, vol. 33, no. S1, pp. 150–161, 2010.

[13] W. E. Farrell, "Deformation of the Earth by surface loads," *Rev. Geophys.*, vol. 10, no. 3, pp. 761–797, 1972.

[14] P. Ferrage, "Jason1&2: Description of the quaternion and solar panel files," Ed.1, Rev. 0. SALP-IF-M/IDS-EA-15938-CN, CNES, 2009. ftp://ftp.ids-doris.org/pub/ids/ancillary/quaternions/jason1_2_quaternion_solar_panel.pdf

[15] C. Flohrer, M. Otten, T. Springer, J. Dow, "Generating precise and homogeneous orbits for Jason-1 and Jason-2," *Adv. Space Res.*, vol. 48, no. 1, pp. 152–172, 2011.

[16] C. Förste, S. L. Bruinsma, S. Rudenko, O. Abrikosov, J.-M. Lemoine, J.-C. Marty, K.-H. Neumayer, R. Biancale, "EIGEN-6S4 – A time-variable satellite-only gravity field model to d/o 300 based on LAGEOS, GRACE and GOCE data from the collaboration of GFZ Potsdam and GRGS Toulouse," GFZ Data Services, 2016. http://doi.org/10.5880/icgem.2016.004

[17] W. M. Folkner, J. G. Williams, D. H. Boggs, "The Planetary and Lunar Ephemeris DE421," IPN Progress Report 42-178, August 15, 2009, 34 pp., 2009. http://ipnpr.jpl.nasa.gov/progress_report/42-178/178C.pdf

[18] H. S. Hopfield, "Two-quadratic tropospheric refractivity profile for correction satellite data," *J. Geophys. Res.*, vol. 74, no. 18, pp. 4487–4499, 1969.
[19] IERS Conventions (2010). G. Petit and B. Luzum (Eds.). IERS Technical Note No. 36, Verlag des Bundesamts für Kartographie und Geodäsie, Frankfurt am Main, 2010. ISBN 978-3-89888-989-6.
[20] J. Kouba, "Implementing and testing of the gridded Vienna Mapping Function 1 (VMF1)," *J. Geod.*, vol. 82, no. 4, pp. 193–205, 2008.
[21] F. G. Lemoine, N. P. Zelensky, D. S. Chinn, D. E. Pavlis, D. D. Rowlands, B. D. Beckley, S. B. Luthcke, P. Willis, M. Ziebart, A. Sibthorpe, J. P. Boy, V. Luceri, "Towards development of a consistent orbit series for TOPEX, Jason-1, and Jason-2," *Adv. Space Res.*, vol. 46, no. 12, pp. 1513–1540, 2010.
[22] J. M. Lemoine, H. Capdeville, "A corrective model for Jason-1 DORIS Doppler data in relation to the South Atlantic Anomaly," *J. Geod.*, vol. 80, no. 8-11, pp. 507–523, 2006.
[23] J.-M. Lemoine, S. Bruinsma, S. Loyer, R. Biancale, J.-C. Marty, F. Perosanz, G. Balmino, "Temporal gravity field models inferred from GRACE data," *Adv. Space Res.*, vol. 39, no. 10, pp. 1620–1629, 2007.
[24] T. Letellier, "Etude des ondes de marée sur les plateux continentaux," Thèse doctorale, Université de Toulouse III, Ecole Doctorale des Sciences de l'Univers, de l'Environnement et de l'Espace, 237 pp., 2004. (In French).
[25] J. W. Marini, "Correction of satellite tracking data for an arbitrary tropospheric profile," *Radio Sci.*, vol. 7, pp. 223–231, 1972.
[26] T. Mayer-Guerr, R. Savcenko, W. Bosch, I. Daras, F. Flechtner, C. Dahle, "Ocean tides from satellite altimetry and GRACE," *J. Geodyn.*, vol. 59–60, pp. 28–38, 2012.
[27] D. D. McCarthy and G. Petit, "IERS Conventions (2003), IERS Technical Note 32," Frankfurt am Main: Verlag des Bundesamts für Kartographie und Geodäsie, 127 pp., paperback, ISBN 3-89888-884-3 (print version), 2004.
[28] OSTM/Jason-2 Products Handbook, 2015. http://www.aviso.oceanobs.com/fileadmin/documents/data/tools/hdbk_j2.pdf.
[29] E. C. Pavlis, "SLRF2008: The ILRS reference frame for SLR POD contributed to ITRF2008", Ocean Surface Topography Science Team 2009 meeting, Seattle, Washington, June 22–24, 2009, http://www.aviso.oceanobs.com/fileadmin/documents/OSTST/2009/poster/Pavlis_2.pdf
[30] M. R. Pearlman, J. J. Degnan, J. M. Bosworth, "The International Laser Ranging Service," *Adv. Space Res.*, vol. 30, no. 2, pp. 135–143, 2002.
[31] P. Rebischung, J. Griffiths, J. Ray, R. Schmid, X. Collilieux, B. Garayt, "IGS08: the IGS realization of ITRF2008," *GPS Solut.*, vol. 16, pp. 483–494, 2012.
[32] S. Rudenko, M. Otten, P. Visser, R. Scharroo, T. Schöne, S. Esselborn, "New improved orbit solutions for the ERS-1 and ERS-2 satellites," *Adv. Space Res.*, vol. 49, no. 8, pp. 1229–1244, 2012.
[33] S. Rudenko, D. Dettmering, S. Esselborn, T. Schöne, Ch. Förste, J.-M. Lemoine, M. Ablain, D. Alexandre, K.-H. Neumayer, "Influence of time variable geopotential models on precise orbits of altimetry satellites, global and regional mean sea level trends," *Adv. Space Res.*, vol. 54, no. 1, pp. 92–118, 2014.
[34] S. Rudenko, D. Dettmering, S. Esselborn, E. Fagiolini, T. Schöne, "Impact of Atmospheric and Oceanic De-aliasing Level-1B (AOD1B) products on precise orbits of altimetry satellites and altimetry results," *Geophys. J. Int.*, vol. 204, no. 3, pp. 1695–1702, 2016.
[35] R. Savcenko and W. Bosch, "EOT11a – Empirical ocean tide model from multi-mission satellite altimetry," Deutsches Geodätisches Forschungsinstitut (DGFI), München, 89, 49 pp., 2012. hdl:10013/epic.43894.d001
[36] T. Schöne, S. Esselborn, S. Rudenko, J.-C. Raimondo, "Radar altimetry derived sea level anomalies – the benefit of new orbits and harmonization," in *System Earth via Geodetic-Geophysical Space Techniques*, F. Flechtner, T. Gruber, A. Güntner, M. Mandea, M. Rothacher, T. Schöne, J. Wickert, Eds., Springer, pp. 317–324, 2010.
[37] B. Tapley, J. Ries, S. Bettadpur, D. Chambers, M. Cheng, F. Condi, B. Gunter, Z. Kang, P. Nagel, R. Pastor, T. Pekker, S. Poole, F. Wang, "GGM02: an improved Earth gravity field model from GRACE," *J. Geod.*, vol. 79, pp. 467–478, 2005.
[38] P. Willis, H. Fagard, P. Ferrage, F. G. Lemoine, C. E. Noll, R. Noomen, M. Otten, J. C. Ries, M. Rothacher, L. Soudarin, G. Tavernier, J. J. Valette, "The International DORIS Service, toward maturity," *Adv. Space Res.*, vol. 45, no. 12, pp. 1408–1420, 2010.
[39] P. Willis, N. P. Zelensky, J. Ries, L. Soudarin, L. Cerri, G. Moreaux, F. G. Lemoine, M. Otten, D. F. Argus, M. B. Heflin, "DPOD2008, a DORIS-oriented terrestrial reference frame for precise orbit determination," IAG Symposia series, 143, 175–181, doi:10.1007/1345_2015_125, 2016.
[40] P. Willis, M. B. Heflin, B. J. Haines, Y. E. Bar-Sever, W. I. Bertiger, M. Mandea, "Is the Jason-2 DORIS oscillator also affected by the South Atlantic Anomaly?" *Adv. Space Res.*, in press, http://dx.doi.org/10.1016/j.asr.2016.09.015, 2016.
[41] S. Zhu, C. Reigber, R. König, "Integrated adjustment of CHAMP, GRACE, and GPS data," *J. Geod.*, vol. 78, no. 1-2, pp. 103–108, 2004.

Sergei Rudenko received Diploma in Astronomy from Leningrad State University, Leningrad, Russia and Ph.D. degree in Physics and Mathematics from the Main Astronomical Observatory of the National Academy of Sciences of Ukraine, Kiev, Ukraine, in 1988 and 2000, respectively. He was a Research Scientist at GFZ German Research Centre for Geosciences (2001-2016). Since 2016, he is a Research Associate at the German Geodetic Research Institute (Deutsches Geodätisches Forschungsinstitut, DGFI) of the Technical University of Munich, Munich, Germany. His main research interests include space geodesy, precise orbit determination of the Earth's artificial satellites, studies on sea level change, Earth gravity field investigations, and studies on the Earth rotation and reference frames.

Karl-Hans Neumayer received the Ph.D. degree in geosciences from Technical University of Munich, Munich, Germany in 1995. Since 2002, he is a Research Scientist at GFZ German Research Centre for Geosciences. His main fields of research include space geodesy, Earth science, gravity field determination, general relativity, mathematics, software development.

Denise Dettmering received the M.Sc. degree in geodesy from the University of Hannover, Hanover, Germany and the Ph.D. degree in geodesy from the University of Stuttgart, Stuttgart, Germany, in 1997 and 2003, respectively. Since 2007, she is with the German Geodetic Research Institute (Deutsches Geodätisches Forschungsinstitut, DGFI), which is a part of the Technical University of Munich (TUM, Munich, Germany) since 2015. Currently, she is head of the satellite altimetry group at DGFI-TUM. Her research interests include multi-mission satellite radar altimetry for sea level and inland water applications, ionosphere modelling, as well as marine gravity field determination.

Saskia Esselborn received the Diploma in Physical Oceanography and the Ph.D. (Dr. rer. nat.) degree in Geoscience and Climate Studies from the University of Hamburg, Hamburg, Germany, in 1995 and 2001, respectively. She was a Research Associate at the University of Hamburg (1995–2000) and a Postdoctoral Researcher at GKSS Research Centre Geesthacht, Institute for Coastal Research (2000–2002). Since 2002, she is with GFZ Helmholtz Centre Potsdam. Her main research interests include satellite altimetry over the ocean and inland waters, implementation and analysis of correction models for satellite altimetry, study of global and regional sea level variability, including steric and mass contributions, processing and analysis of GRACE data over the ocean, and analysis of tide gauge data.

Tilo Schöne received the Ph.D. degree in geosciences from University of Bremen in 1997. He was with Alfred Wegener Institute for Polar and Marine Research (1991–1999). Since 1999, he is with GFZ German Research Centre for Geosciences. His main research topics include sea level change, tsunamis, tide gauges, GPS analyses at tide gauges, geodetic off-shore technology, high-altitude monitoring stations, sea level related hazard monitoring. Dr. Schöne is a member of the International GNSS Service (IGS) Governing Board, the Chair of the IGS Tide Gauge Benchmark Monitoring (TIGA) working group, and a member of the Global Geodetic Observing System (GGOS) Coordinating Board.

Jean-Claude Raimondo received his education in aerodynamics and fluid mechanics at Universite de Provence, Marseille, France in 1973. He received master of sciences in aeronautics and astronautics at the University of Washington in Seattle, USA and master of sciences in aerospace engineering at the University of Texas at Austin in 1975 and 1983, respectively. He was a Scientist at Deutsches Geodätisches Forschungsinstitut (DGFI), Munich, Germany (1983–1992). He has been a Scientist at GFZ German Research Centre for Geosciences (1992-2013). Since 2014, he is with SpaceTech GmbH, Immenstaad, Germany. His main research interests include space geodesy, precise orbit determination, gravity field determination, next generation gravity mission simulations, as well as software development.